

this mixed gradient term vanishes and an imaginary combination d_{\pm} is required to minimize the free energy. As a result, we find

$$J_y = 4e_v \text{Im} (s_{\pm} c_{x-d} + d_{\pm} c_{x-s}); \quad (3)$$

note $[J_x = 4e_v \text{Im} (s_{\pm} s_{\pm} c_{x-s} + d_{\pm} d_{\pm} c_{y-d})]$ is identically zero]. Away from the surface towards the bulk, the d-wave component saturates and the s-wave component decays to zero. Thus the parallel spontaneous supercurrent is limited to the surface region. The detailed value of J_y must be obtained by solving the GL equation for s_{\pm} and d_{\pm} subject to the appropriate boundary conditions. However, the knowledge of J_y will not provide the information for the flow pattern since the supercurrent must circulate as loops in a realistic two dimensional system. The investigation of supercurrent flow is a challenging topic, it is difficult to employ the GL theory or other continuum theories to examine this problem. The exact diagonalization approach can attack this problem in an elegant way. In addition, the band structure and the short coherence length effects can also be incorporated. The weakness is that the finite size exact diagonalization method, if without modification, lacks the spectral resolution to resolve the resonances in energy. However, for the order parameter and the current (will be calculated below) the finite size effect is small since these two physical quantities are determined by the local pairing interaction and local hopping integral, respectively.

Within an extended Hubbard model, the Bogoliubov-de Gennes (BdG) [20] equations can be written as:

$$\sum_j \begin{pmatrix} H_{ij} & t_{ij} \\ t_{ji}^* & H_{ij} \end{pmatrix} \begin{pmatrix} u_j^n \\ v_j^n \end{pmatrix} = E_n \begin{pmatrix} u_i^n \\ v_i^n \end{pmatrix}; \quad (4)$$

where u_i^n and v_i^n are the Bogoliubov amplitudes at site i with eigenvalue E_n , and

$$H_{ij} = t_{i\pm j} + (U_i - t_{i\pm j}) \delta_{ij}; \quad (5)$$

$$t_{ij} = t_0 \delta_{ij} + t_1 (\hat{x}_{ij} + \hat{y}_{ij}); \quad (6)$$

Here we choose the x and y axes to lie on the diagonals of the sample [as shown in Fig. 1], and \hat{x} ; \hat{y} are the nearest-neighbor vectors along the x and y axes, t is the hopping integral, U_i is introduced to represent the impurity scattering potential. The energy gaps for on-site and nearest-neighbor pairing are determined self-consistently

$$\Delta_0(i) = V_0 \sum_n u_i^n v_i^n / \tanh(E_n/2T); \quad (7)$$

$$\Delta_{\pm}(i) = \frac{V_1}{2} \sum_n [u_i^n v_{i\pm}^n + u_{i\pm}^n v_i^n] \tanh(E_n/2T); \quad (8)$$

where V_0 and V_1 are on-site and nearest-neighbor interaction strength, respectively. Positive values of V_0 and

V_1 mean attractive interactions and negative values mean repulsive interactions. In terms of the Bogoliubov amplitudes, the average current from site j to i is given by

$$J_{ij} = \frac{2ie\hbar}{h} \sum_n f(E_n) u_i^n u_j^n + (1 - f(E_n)) v_i^n v_j^n \cdot c_{ij}; \quad (9)$$

where the prefactor comes from the spin degeneracy and $f(E) = [\exp(E/T) + 1]^{-1}$ is the Fermi distribution function.

We solve the BdG equations (4) self-consistently [21]. Throughout the work, we take $V_1 = 3t$, $t = t$. This set of parameter values give $t_d = 0.368t$, $T_c = 0.569t$, and the corresponding coherence length $\xi_0 = \hbar v_F / \Delta_d = 3a$ (In YBCO, $\xi_0 = 15 \text{ \AA}$). As a model calculation, the value of hopping integral t will be adjusted to give a reasonable transition temperature. The amplitudes of the d- and the induced s-wave order parameters are defined as:

$$d_{\pm}(i) = \frac{1}{4} [\hat{x}_{\pm}(i) + \hat{x}_{\pm}(i) \mp \hat{y}_{\pm}(i) \mp \hat{y}_{\pm}(i)]; \quad (10a)$$

$$s_{\pm}(i) = \frac{1}{4} [\hat{x}_{\pm}(i) + \hat{x}_{\pm}(i) + \hat{y}_{\pm}(i) + \hat{y}_{\pm}(i)]; \quad (10b)$$

In general, both components are complex, i.e., $d_{\pm}(i) = |d_{\pm}(i)| \exp(i\phi_{\pm}(i))$ with $\phi_{\pm}(i) \in [0, 2\pi]$. Their relative phase is defined as $\phi = \phi_s - \phi_d$. We first study the spatial variation of s-wave and d-wave order parameter and the relative phase in a square d-wave superconductor having f110g-oriented boundaries. The obtained current distribution is drawn in Fig. 1. The current direction is denoted by the arrows in the figure. This calculation is made under the open boundary condition for a clean sample of size $10^2 a \times 10^2 a$, $T = 0.02t$ and $V_0 = t$. We

find that the d-wave order parameter is suppressed near the boundary and approaches to the bulk value beyond a coherence length scale ξ_0 . The induced s-wave component near the boundary oscillates at an atomic scale and decays to zero in the bulk region at a distance of a few coherence lengths. Near the four corners of the sample, the d-wave component is more strongly suppressed while the magnitude of induced s-wave component is enhanced. Our numerical calculation shows that if the order parameter at site j within square O H A B (see Fig. 1) is $d_{\pm} = d_r + id_i$ and $s_{\pm} = s_r + is_i$ [for definiteness, $d_{r,i}$ and $s_{r,i}$ are taken to be positive], then at site j' within square O H G F which is related to site j by a $\pi/2$ rotation around the origin O, the order parameter can be obtained as $d_{\pm} = d_r + id_i$ and $s_{\pm} = s_r + is_i$. Correspondingly, the relative phase is $\phi = 2\pi + \phi$ at site j and $\phi = 2\pi + \phi$ at site j' , where $\phi = \tan^{-1}(s_i/s_r) - \tan^{-1}(d_i/d_r)$ is site dependent. On the $\hat{x}j = \hat{y}j$ lines [the dotted lines in Fig. 1], $\phi = 0$ and the order parameter becomes exactly d_{\pm} is. Therefore, the pairing state in a square d-wave superconductor with f110g-oriented boundaries is a BTRS $d_{\pm} + e^{\pm i\phi}$ state with varying spatially, and the existence

of the BTRS state is limited within a region of the order of ξ_0 near the sample edges. We have also found that the induced s-wave component of order parameter decreases with increasing temperature and on-site repulsive interaction. For a given on-site interaction $V_0 = t$, the s-component of the surface pairing state vanishes at a temperature about $0.1T_c$ [21]. In our lattice model, the current flows into (or out of) each lattice site connecting four bonds. The current conservation on each site is respected. As it can be seen from Fig. 1, the current flowing at four edges, AC, CE, EG, and GA, does not form a closed loop to surround the whole sample. Instead, the current distribution has a spatial reflection symmetry with respect to the x and y axis. Current flows pointing to the corners on the x axis but away from the corners on the y axis. At the left and right corners, the current flowing in the x direction is separated into two equal branches, which flow in the positive and negative y direction; while at the upper and lower corners, the current flowing in the y direction consists of two equal parts flowing in the positive and negative x direction. From an overall point of view, current flows clockwise or counterclockwise in four triangles separated by the x and y axes [i.e., OAC, OAG, OGE, OEC]. Correspondingly, the total flux in two nearest-neighbor triangles for example OAC and OAG has opposite signs. In the upper-right inset of Fig. 1, we indicate the direction of flux in each triangle. In contrast to the regular diamagnetic Meissner current which flows in a penetration depth, the spontaneous current is confined to a distance of a few ξ_0 from the sample edge because it is determined by the spatial variation of order parameter.

To calculate the flux in each triangle, we use the Maxwell equation, $\nabla \times \mathbf{B} = (4\pi/c)\mathbf{J}$, which relates the magnetic field \mathbf{B} to the current density \mathbf{J} . By assuming that the lattice spacing between two consecutive superconducting layers is c_0 , the Maxwell equation can be written as

$$\frac{4}{c} J_{ij} = \frac{c_0}{a^2} (\phi_i - \phi_j); \quad (11)$$

where if ij is a horizontal link from left to right, ϕ_i and ϕ_j are respectively the magnetic flux passing through the upper and lower plaquettes with the link ij as a common boundary. The magnetic field and the corresponding flux is perpendicular to the lattice plane since both the current J_{ij} and the vector connecting the centers of two plaquettes are in the plane. The flux carried by a vortex is then obtained by summing over the flux encircled by each plaquette in a triangle. Using the calculated current distribution to solve Eq. (11), the flux in the triangle AOC is found to be $\phi = \phi_i - \phi_j = 1.2LI_0$, where $L = 4a^2/c_0$ and $I_0 = et/h$. For $t = 0.014$ eV which gives $T_c = 92.4$ K, and $a = 4$ Å and $c_0 = 10$ Å, we have $\phi = 4.04 \times 10^{-7} \phi_0$, where $\phi_0 = 2.07 \times 10^{-7}$ G Å² is the superconducting flux quantum. Due to the small size we consider, the

value is too small to be measurable.

To measure the spontaneous flux as an evidence for the BTRS pairing state, we propose the following experiment. Create several long defect lines in a single crystal of d-wave superconductor. These lines lie parallel to the same f110g direction. To give a detailed analysis, we consider three parallel f110g-oriented defect lines in the sample of size $100\sqrt{2}a \times 100\sqrt{2}a$. The width of them is $\sqrt{2}a$, $\sqrt{2}a$, and $3\sqrt{2}a$. The centers of the defect lines are located at $60a = \sqrt{2}$, $101a = \sqrt{2}$, $159.5a = \sqrt{2}$. Therefore, the distance between the edges of two consecutive lines are, $39a = \sqrt{2}$, $56a = \sqrt{2}$, respectively. In the numerical calculation, we use the single-site potential of strength $U = 100t$ to model the defect lines, and impose the periodic boundary condition to focus on the physical properties associated with the defect lines. The spatial dependence of the order parameter and spontaneous current are shown in Fig. 2. As expected, when the dominant d-wave order parameter is suppressed near the defect lines, the s-wave order parameter is admixed with a relative phase $\pi/2$ with respect to the d-wave order parameter. More importantly, the admixture of the s-wave and d-wave components is globally d₊ is: The relative phase is the same not only on the left and right sides of each defect line (i.e., d₊ is and d₊ is) but also near all defect lines. For the profile of the s-admixture near a defect line, a similar result that the relative phase is the same on both sides of a f110g-oriented boundary coupling two d-wave superconductors was obtained based on the quasi-classical theory [10]. The same admixture of the s-wave component (i.e., d₊ is) on the two edges of a superconducting segment created by two consecutive defect lines, which comes from a small overlap of the electron wavefunctions at two defect lines, can gain more condensation energy. If the s-wave admixture became d₊ is at one edge and d₋ is at the other, there would be a π -phase jump in the middle region of the superconducting segment, which is physically unacceptable. More recently, it has also been found [22] that an s-wave component is admixed with the same sign on both sides of a f110g-oriented d-wave superconducting strip. This strip is in geometry similar to the superconducting segment we are considering here. As a consequence, the spontaneous currents flowing at the left and right sides of each defect line have opposite directions. In this respect, the system under consideration is different from an s-wave/normal metal/d-wave superconductor junction [23], where the BTRS pairing state appears in the normal metal, and the spontaneous supercurrent has the same direction so that the generated magnetic flux has opposite sign across the corresponding region. In addition, our results show that the current profile near all defect lines is the same. With the above observation, the magnetic field induced by the current near these defect lines has the same direction. If the pairing state is d₋ is, the directions of the current and magnetic field are globally reversed. As shown in Fig. 2,

our results are independent of the width of and the distance between the defect lines. Moreover, if the distance between the defect lines is of several coherence lengths, the contribution to the magnetic flux from each defect line is almost the same. With the chosen values of structure parameter, the flux contribution from a single defect line of length $30 \mu\text{m}$ is estimated to be $3.4\% \Phi_0$. If twenty such defect lines are introduced into the sample, the total flux can be as large as $68\% \Phi_0$. In this sense, the effect of BTRS pairing state is greatly amplified whereas the information from the tunneling spectroscopy is determined by the local property near one individual defect line or surface. We suggest to use the heavy-ion bombardment technique [24] to realize the desired arrangement of the defect lines. With this technique, the edge of the defect line can also be very sharp so that it has a well defined in-plane orientation. The magnetic flux can then be measured by a SQUID microscope through a pickup loop [25]. Here the pickup loop should be constructed to cover the central part of all defect lines. Since the proposed experiment does not involve as-grown grain boundaries or twin boundaries, the existence of a spontaneous flux would be a direct evidence for the BTRS pairing state.

We would like to thank Dr. C. C. Tsuei for useful discussions. This work was supported by the Texas Center for Superconductivity at the University of Houston, by the Robert A. Welch Foundation, and by the grant NSF-INT-9724809.

[1] C. R. Hu, Phys. Rev. Lett. 72, 1526 (1994).
[2] Y. Tanaka and S. Kashiwaya, Phys. Rev. Lett. 74, 3451 (1995).
[3] J. H. Xu, J. H. Miller, and C. S. Ting, Phys. Rev. B 53, 3604 (1996).
[4] J. Geerk, X. X. Xi, and G. Linker, Z. Phys. B 73, 329 (1988).
[5] J. Lesueur et al., Physica (Amsterdam) 191C, 325 (1992).
[6] M. Covington et al., Appl. Phys. Lett. 68, 1717 (1996).
[7] For a review see M. Sigrist, Prog. Theor. Phys. 99, 899 (1998).
[8] M. Sigrist, D. B. Bailey, and R. B. Laughlin, Phys. Rev. Lett. 74, 3249 (1995).
[9] L. J. Buchholtz et al., J. Low Temp. Phys. 101, 1079 (1995); 101, 1099 (1995).
[10] M. Matsumoto and H. Shiba, J. Phys. Soc. Jpn. 64, 3384 (1995); 64, 4867 (1995); 65, 2194 (1996).
[11] M. Sigrist et al., Phys. Rev. Lett. 53, 2835 (1996).
[12] D. L. Feder et al., Phys. Rev. B 56, R5751 (1997).
[13] W. Belzig, C. Bruder, and M. Sigrist, Phys. Rev. Lett. 80, 4285 (1998).
[14] M. Fogelstrom and S.-K. Yip, Phys. Rev. B 57, R14060 (1998); Y. Tanaka and S. Kashiwaya, Phys. Rev. B 58,

R2948 (1998).
[15] M. Covington et al., Phys. Rev. Lett. 79, 277 (1997).
[16] M. Fogelstrom, D. Rainer, and J. A. Sauls, Phys. Rev. Lett. 79, 281 (1997).
[17] S. Sinha and K.-W. Ng, Phys. Rev. Lett. 80, 1296 (1998).
[18] A. Engelhardt, R. Dittman, A. I. Braginski, Phys. Rev. B (submitted).
[19] J. Y. T. Wei et al., Phys. Rev. Lett. 81, 2542 (1998).
[20] P. G. de Gennes, Superconductivity of Metals and Alloys (Benjamin, New York, 1966).
[21] The numerical method has been described clearly in, Jian-Xin Zhu, B. Friedman, C. S. Ting, Phys. Rev. B 59, 3353 (1999).
[22] C. Honerkamp, K. Wakabayashi, and M. Sigrist, cond-mat/9902026; C. Honerkamp, private communication.
[23] A. Huck, A. v. Otterlo, and M. Sigrist, Phys. Rev. B 56, 14163 (1997).
[24] H. Walter et al., Phys. Rev. Lett. 80, 3598 (1998).
[25] J. R. Kirtley et al., Phys. Rev. B 51, 12057 (1995).

FIG. 1. The current distribution in a square d-wave superconductor with $110g$ boundaries. The current direction is represented with arrows. The value of parameters used in the calculation are $T = 0.02t$ and $V_0 = t$. The upper-right inset shows the direction of flux in each triangle.

FIG. 2. The spatial variation of the order parameter (a) and the spontaneous current (b) in a $100^{\circ}2a \times 100^{\circ}2a$ sample containing three defect lines parallel to the $110g$ direction. The solid line (with filled square) corresponds to the d-wave component and the dotted line (with empty square) to the s-wave component. Here the distance is measured in units of $a^0 = a/\sqrt{2}$.

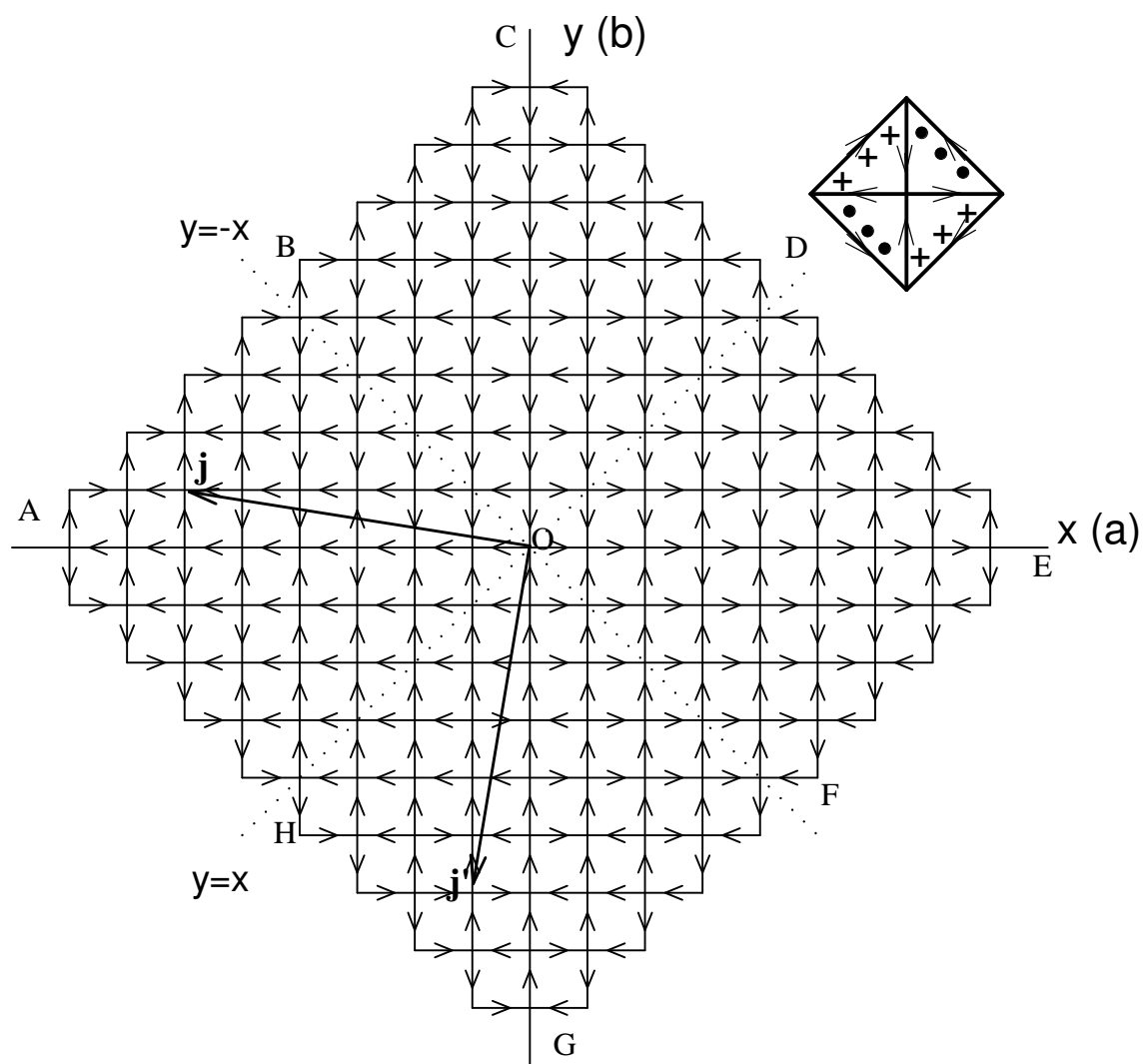


FIG. 1 Zhu et al.

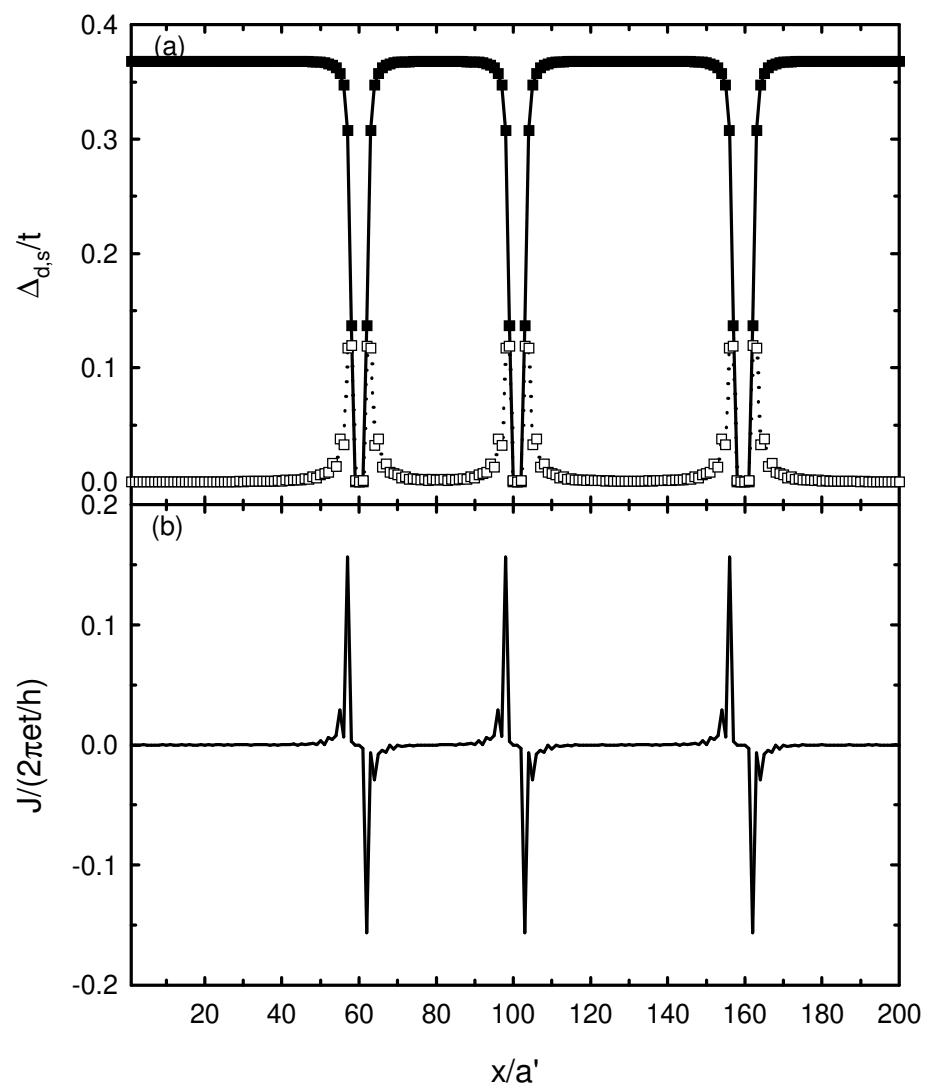


FIG. 2 Zhu et al.

